# 11A.3 THE ESTIMATION OF X-BAND ATTENUATION DUE TO WET ICE IN THE MIXED PHASE REGION OF CONVECTIVE STORMS AND CORRECTION OF LDR AT X-BAND USING THE CP-2 RADAR

V.N. Bringi[1] and Gwo-Jong Huang[1]
Peter May[2], Ken Glasson[2] and Thomas Keenan[2]

[1]Colorado State University, Fort Collins, Colorado, USA
[2] Centre for Australian Weather and Climate Research, Melbourne, Australia

## 1. INTRODUCTION

It is well known that high frequency radar (C-band and above) signals suffer from significant attenuation when the propagation path intercepts convective rain cells. Subsequently, radar measurements which relate to received power such as the radar reflectivity factor ($Z_{h,v}$), differential reflectivity ($Z_{dr}$) as well as the linear depolarization ratio (*LDR*) must be corrected for rain attenuation. Two common methods to correct for rain attenuation are to relate the specific attenuation ($A$) to specific differential phase ($K_{dp}$) or $Z_h$ in the power-law form (Bringi et al. 1990; Hitschfeld and Bordan 1954). However, in the mixed phase region which includes supercooled rain drops and wet graupel/hail in the temperature around +5$^o$ to -10$^o$ C, the $K_{dp}$ is not sensitive to the nearly isotropic wet ice particles, and the coefficient of the *A-Z* relationship is strongly dependent on the unknown water fraction of the precipitation. Therefore, we need a method which can measure the attenuation directly.

One method used in the early '70s was the dual-wavelength radar using the non-attenuated S-band radar (as a reference) along with an X-band radar, both radar beams being well matched and aligned (Eccles and Mueller 1971). The CP2 radar operated by NCAR along with the CHILL radar played important roles in hail detection by making use of the Mie scattering at X-band due to hail particles > 1 cm or so. Later in the early 1980s, the CP2 radar was modified for dual-polarization measurements in addition to dual-wavelength measurements. For a full description of the CP-2 radar circa 1990 see Bringi and Hendry (1990). The radar has subsequently been used in the same configuration in Florida during CaPE and SCMS during the early and mid '90s (Bringi et al 1997; Knight and Miller 1998).

* Corresponding author address: V.N. Bringi, Dept. of ECE, Colorado State University, Fort Collins, CO 80523
e-mail: bringi@engr.colostate.edu

Currently, the CP-2 radar is located SW of Brisbane, Australia (see Fig. 1), and has been operated by the Centre for Australian and Climate research since late 2007 in collaboration with NCAR. This unique radar, with its new signal processor developed at NCAR, can now, for the first time, measure the differential propagation phase ($\Phi_{dp}$) and the copolar correlation coefficient ($\rho_{hv}$) at S-band. The original fields such as the *DWR*, *LDR* (at X-band), $Z_{dr}$ (at S-band) and so on are still maintained. A report on the initial radar data quality was prepared by Bringi and Thurai (2008).


Fig. 1: The CP2 radar is located by the "red +" mark to the SW of Brisbane.

In this paper, we use the *DWR* to estimate the total specific attenuation ($A_{total}$) at X-band. In the mixed phase region of rapidly developing convective storms, the rain component of this attenuation ($A_{rain}$) can be derived from the S-band $K_{dp}$, and then, the specific attenuation due to the wet ice ($A_{ice}$) is the difference between the

$A_{total}$ and the $A_{rain}$. As a further application, we propose a new scheme of using the $A_{total}$ to correct the measured *LDR* which suffers from one-way differential attenuation ($A_{dp}$) between the H and V-polarizations which is apparent as a rapid increase in measured *LDR* along the beam in moderate-to-intense rain.

## 2. THEORETICAL BACKGROUND

### 2.1 Dual-wavelength reflectivity ratio

As mentioned earlier, the DWR has been used since the early '70s to detect hail larger than about 1 cm (Mie scattering at X-band) as well as to estimate the attenuation due to rain (e.g., Tuttle and Rinehart 1983). The DWR is defined defined as:

$$DWR = Z_s^m - Z_x^m \quad \ldots\ldots\ldots (1)$$

where $Z_s^m$ and $Z_x^m$ are the radar reflectivities measured at S/X-band in units of dBZ. The $Z_s^m$ is proportional to $|S_{hh}^s|^2$ whereas $Z_x^m$ is proportional to $|S_{hh}^x|^2$ less the 2-way path attenuation. It is easy to show that *DWR* can be expressed as:

$$DWR(r) = PIA_x(r) + HS(r) \quad \ldots\ldots (2)$$

where $PIA_x$ is the two-way path-integrated attenuation at X-band:

$$PIA_x(r_1) = 2\int_{r_0}^{r_1} A_x(r)dr \quad \ldots\ldots\ldots (3)$$

and *HS* is the hail signal due to the Mie scattering at X-band given as $10log_{10}[|S_{hh}^s|^2 \div |S_{hh}^x|^2]$.

To separate the *PIA* and *HS* from the *DWR*, we use an iterative FIR range filter technique proposed by Hubbert et al. (1995). This technique was originally developed for separating the differential propagation phase ($\Phi_{dp}$) and differential scattering phase ($\delta$) from measured differential phase ($\Psi_{dp}$). Since the mathematical form of $\Psi_{dp}(\Phi_{dp},\delta)$ is the same as *DWR*(*PIA*,*HS*), the iterative FIR range filtering technique can also be used for *DWR data* (as was shown by Hubbert et al. 1995 using CP-2 data).

The upper panel of Fig. 2 shows a typical range profile of measured $Z_h$ at two frequencies (S- and X-band). The *DWR* (the blue line in the bottom panel) is computed by subtracting $Z_x$ from $Z_s$. After applying the iterative FIR range filter, we can get the smoothed *PIA* (red line in bottom panel) and *HS* (the difference between *DWR* and smoothed *PIA*). Since the strong *HS* appears near the end of filtering range (40 to 43km; note the magenta circle), it may be due to either the edge effect of the filter or large ice particles. Therefore, we computed the hail detection ratio (*HDR;* Aydin et al. 1986 ) to verify the results. The *HDR* values in this range interval are larger than 13 dB with peak of 20 dB at 41 km. It implies that it is a physically meaningful hail signal. Finally, the total specific attenuation can be computed as:

$$A_{total} = \frac{1}{2}\frac{d}{dr}PIA \quad \ldots\ldots\ldots (4)$$

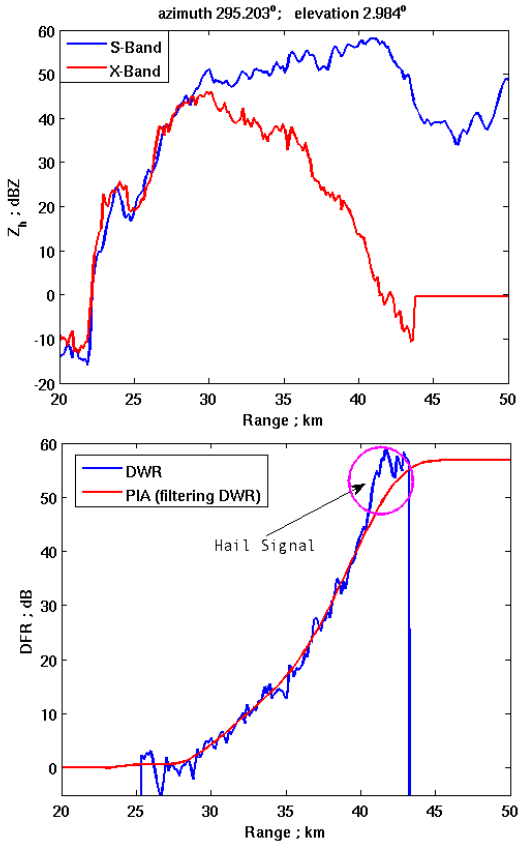


Fig. 2: A typical range profile of (top panel) $Z_h$ at S (blue) and X-bands (red) where the latter is strongly attenuated by more than 50 dB. Case is from 26 March, 2008 in deep convection. Bottom panel shows *DWR* in 'blue' and the iteratively filtered version (in 'red'). Note that inside the magenta circle (40-43 km) a strong hail signal (*HS*), can be noted; the corresponding HDR there is larger than 13 dB (peak ~20 dB).

## 2.2 Correcting *LDR*

The X-band measured *LDR* will be significantly biased due to differential attenuation between the H and V polarized signals. In the case of CP-2, the transmitted polarization for the X-band channel is H only. There are two antennas, one receives the H and the other the V component of the back scattered signal. In this case the measured LDR will increase with increasing penetration into the rain medium (see Chapter 4 of Bringi and Chandrasekar 2001). Theoretically, there is a linear relation between *A* and $A_{dp}$ as $A_{dp} = \gamma * A$ in rain. Here A refers to the specific attenuation at H-polarization; the subscript 'H' is dropped for ease of notation. In practice, based on scattering simulations using a wide variety of DSDs, a 'fitted' value of $\gamma$ can be estimated which could lead either to under or over correction of the measured *LDR*. Here, we seek to estimate $\gamma$ from the data itself. The 'true' *LDR* at range *r* can be expressed as:

$$LDR(r) = LDR_m(r) - \int_0^r A_{dp}(s)ds \quad \text{.....(5)}$$

Therefore, the difference in *LDR* between $r_2$ and $r_1$ is given by:

$$\Delta LDR = \Delta LDR_m - \gamma \int_{r_1}^{r_2} A(s)ds \quad \text{.....} \qquad (6)$$

To estimate $\gamma$ we have to make an assumption on the difference between the 'true' *LDR* at the begin and end ranges ($r_1$ *and* $r_2$). Our algorithm attempts to locate $r_1$ as the beginning of a rain cell, and $r_2$ as its end. If light rain exists at $r_1$ and $r_2$, then $\Delta LDR$ should be close to 0 dB and $\gamma$ can be estimated as:

$$\gamma = \frac{\Delta LDR_m}{\frac{1}{2}\Delta PIA} \quad \text{.....} \qquad (7)$$

where $\frac{1}{2}(\Delta PIA)$ is the one-way path-integrated attenuation which can be computed from *DWR*. On the other hand, if part of the radar beam is in the mixed phase region and the rain component of the mixture is large, the $A_{total}$ should be dominated by $A_{rain}$. Then our method of estimating $\gamma$ would still be useful for attenuation-correction. Using (7) as our estimate of $\gamma$, we now can perform the gate-by-gate correction of the measured *LDR* using (5).

Fig. 3 shows a example of *LDR* correction. The measured *LDR* (blue line) shows a significant increase versus range which should be corrected for to estimate the 'true' *LDR* values.

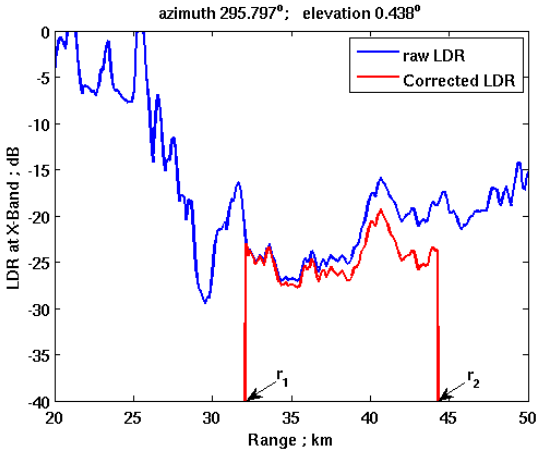


Fig. 3: The range profile of measured *LDR* (blue line) and the corrected *LDR* (red line). The measured *LDR* shows a dramatic increase vs. range which is due to the differential attenuation. Note that the locally enhanced values of *LDR* at around 40 km (around –20 dB) most likely indicates rain mixed with wet ice hydrometeors. .

The locally enhanced values of corrected LDR (-20 dB at 40 km range) likely indicates the presence of wet ice hydrometeors mixed with rain. Note that $r_1$ is decided by, (a) standard deviation of 10 consecutive $\Phi_{dp}$ values < 7.5°, (b) co-polar SNR at X-band > 3 dB, (c) cross-polar SNR at X-band > 3 dB, (d) $LDR(r_1)$ less than -25 dB, and (e) the standard deviation of 5 consecutive *LDR* values < 3 dB. The conditions (a) and (b) ensure the quality of S/X-band $Z_h$ data which are used to compute *DWR*. The conditions (c) – (e) ensure the quality of the X-band *LDR* data. The $r_2$ is usually decided by where the X-band signal falls below noise level (mainly due mainly to strong attenuation). Note that the system LDR limit for the CP-2 radar is close to -31 dB (Bringi and Thurai 2008).

## 3. CASE STUDY

To demonstrate the techniques proposed in this paper, we show data from an intense thunderstorm which occurred on 26 March 2008. The upper panel of Fig. 4 shows S-band $Z_h$ with overlay of contours of X-band total specific attenuation (in black) starting at 1 with steps of 1 dB/km. The bottom panel shows the X-band $Z_h$ which is highly attenuated and losing signal [note 'V' shaped notch starting at around (-32,12 km)].

Fig. 5 shows the vertical sections of $Z_{dr}$ (top) and $K_{dp}$ (bottom) with the contours of S-band $Z_h$. Note the 'V' shaped notch of low $Z_{dr}$ values (0-0.75 dB) within the 50-60 dB reflectivity levels

indicating that the main precipitation shaft centered at 40 km is composed of hail mixed with intense rain rates (high $K_{dp}$ near 4 °/km or 150 mm/h).

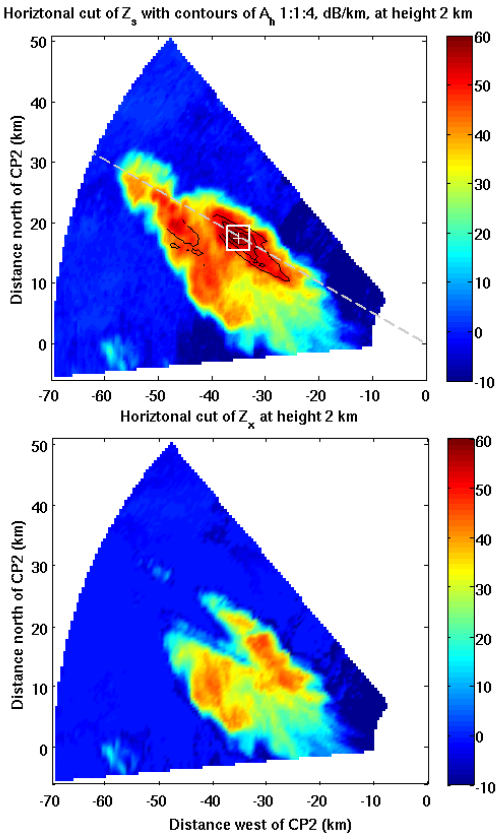


Fig. 4: Horizontal cut of S-band (upper panel) and X-band (bottom panel) $Z_h$ at 2 km height. The thin black lines in the upper panel are the contours of $A_{total}$ starting at 1 with steps of 1dB/km. The white-lined box is the area we have selected to show the averaged vertical profile of specific attenuation (see Figure 7). The grey dash line is the azimuth angle equal to 297° along which we show the vertical section later (see Figures 5 and 6).

The upper panel of Fig. 6 shows the vertical section of $A_h$ derived from the *DWR*. The vertical column of enhanced $A_h$ at range 40 km with the 0.5-1 dB/km contour extending well up to 6 km (-10° C) may be considered the mixed phase region extending through the height interval 3-6 km with the maximum value of 4 dB/km at 1 km height. The middle panel of Fig. 6 shows the 'raw' or measured LDR without any attenuation correction. Note loss of signal at ranges > 45 km. The bottom panel is the vertical section of corrected LDR using the technique discussed in Section 2.2. Note the enhanced values of corrected *LDR* (~ -17 dB) centered around range of 36 km at 5 km height; this is indicative of wet ice hydrometeors (Bringi and Chandrasekar 2001). In (6) the assumption is made that $\Delta LDR = LDR(r_2)-LDR(r_1)$ is nearly 0 dB. This need not be the case if $r_1$ is in rain and $r_2$ in ice. If $\Delta LDR<0$ then no attenuation-correction is made. If $\Delta LDR>0$ then the correction may be over-estimated and the $\gamma$ parameter for the beam can then be interpreted as an 'apparent' $\gamma$ that tends to remove the mean trend of the measured LDR range profile. Later in Fig. 7 we show that the LDR correction scheme gives plausible results below the freezing level (4 km height).

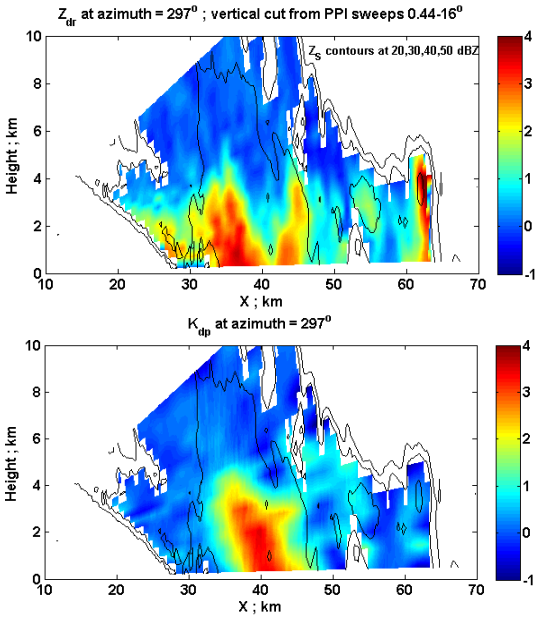


Fig. 5: The color-filled contours of $Z_{dr}$ (upper panel), $K_{dp}$ (bottom panel). The environmental 0° C height is at 4 km and the -10° C at 6 km. The black lines are the contours of S-band $Z_h$ started from 10 dBZ with steps of 10 dBZ

The method of separately estimating the specific attenuation due to rain and wet ice in the mixed phase region involves using the $A_{total}$ and $A_{rain}$ where the latter is estimated from the $K_{dp}$ while the former is estimated from the DWR. There is nearly a 1:1 relation between $A_{rain}$ at X-band and $K_{dp}$ at S-band; however, here we use simulations based a wide variety of DSDs to establish the $A_{rain}$-$K_{dp}$ relation. The wet ice attenuation ($A_{ice}$) is then the difference between $A_{total}$ and $A_{rain}$. The previous radar simulations using the two-moment scheme of the Regional Atmospheric Modeling System (RAMS) of a supercell storm (Leon et al. 2007) showed that the procedure for estimating attenuation due to wet ice in the mixed phase zone could be accurately determined even in the presence of random measurement errors in the $Z_e$ at S/X-bands and in the $K_{dp}$. However, data from the CP-2 radar

shows that such simulated accuracy is difficult to achieve by differencing $A_{total}$ and $A_{rain}$ on a gate-to-gate basis. Recall that $A_{rain}$ is directly related to $K_{dp}$, and that $K_{dp}$ and $A_{total}$ are, respectively, based on the smoothed $\phi_{dp}$ and *DWR* range profiles. The iterative FIR filter used is the same; however, because the *DWR* is from 2 separate radars while the $\phi_{dp}$ is from the same radar, it turns out that the while the range correlation between *DWR* and $\phi_{dp}$ is quite acceptable, the corresponding range correlation between the $A_{total}$ and $K_{dp}$ is less than ideal (because the latter are range derivatives). This is more evident in spatially smaller rain cells (<5-6 km) as opposed to larger more organized convection. This lack of high range correlation precludes the estimation of the wet ice attenuation based on gate-to-gate differencing of $A_{total}$ and $A_{rain}$. Therefore, we use a spatial average over a 4x4 km area centered at the storm core (the white-line box in the top panel of Figure 4) which reduces the error and gives a smoother vertical profile of the wet ice attenuation through the mixed phase region.

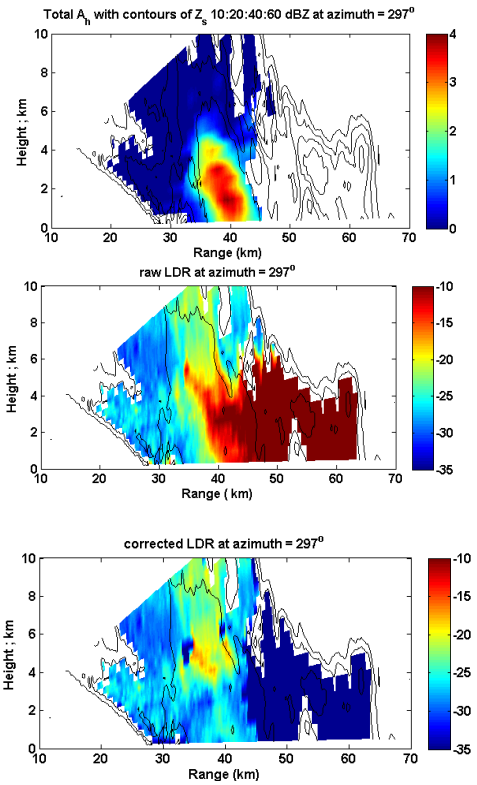


Fig. 6: (upper) The color-filled contours of total specific attenuation derived from *DWR*. The maximum value is 4 dB/km at 1 km height. (middle) 'raw' LDR, i.e., without any attenuation correction; note loss of signal beyond range of 45 km and (bottom) the LDR corrected by $A_h$. Note the high values (around -17 dB at 35 km range and 5 km height) indicative of wet ice hydrometeors.

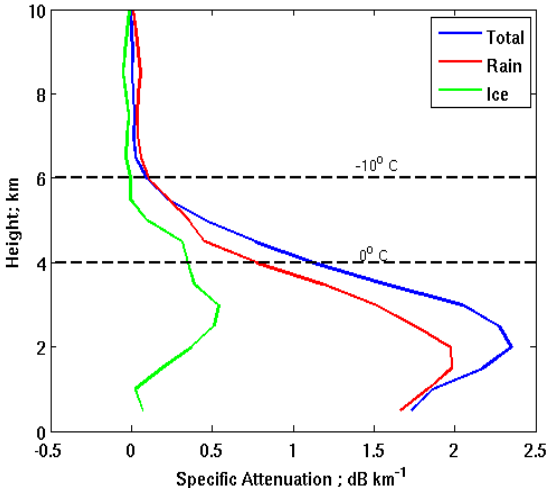


Fig. 7: The averaged vertical profile of specific attenuation. The $A_{total}$ is derived from *DWR*, the $A_{rain}$ is derived from S-band $K_{dp}$, and the $A_{ice}$ is the difference between $A_{total}$ and $A_{rain}$.

Fig. 7 shows the vertical profile of specific attenuation after averaging over the 4X4 km box. It shows that the $A_{total}$ has peak of 2.4 dB/km at 2 km height and the $A_{rain}$ has peak of 1.9 dB/km at the same height. Basically, the total specific attenuation is dominated by the specific attenuation of rain. Also, the $A_{ice}$ increases starting from ~ 2 km and reaches its peak (~ 0.5 dB/km) at 3 km height and continues to have significant values up to 5 km. Hence, in this case the mixed phase region extends from 2 to 5 km.

## 4. Conclusions

A method of separately estimating the specific attenuation at X-band due to wet ice and rain has been developed using the *DWR* and S-band $\phi_{dp}$ data. Moreover, we have also developed a new scheme of correcting *LDR* due to differential attenuation in rain by using the DWR-based estimate of the total attenuation. The addition of these new products, in addition to other measureables make the CP-2 radar a unique and powerful tool for the study of the spatial and temporal variability of the microphysics of convective storms.

## ACKNOWLEDGEMENTS

The CP-2 radar is an operational research system under the Centre for Australian Weather and Climate Research in collaboration with NCAR. VNB and GJH acknowledge support

from the NASA PMM science grants program. Partial travel support for VNB to Australia was provided by the Centre for Australian Weather and Climate Research, Melbourne, AU.

## REFERENCES

Aydin, K., T.A. Seliga and V. Balaji, 1986: Remote Sensing of Hail with a Dual Linear Polarization Radar. *J Appl Meteor.* Vol. 25, pp 1475–1484

Bringi, V.N. and V. Chandrasekar, 2001: *Polarimetric Doppler Weather Radar: Principles and Applications*, Cambridge Univ. Press, pp. 636.

Bringi, V.N. and A. Hendry, 1990: Technology of polarization diversity radars for meteorology. In *Radar in Meteorology*, D. Atlas, Ed., AMS, Boston, MA, pp 1530190.

Bringi, V.N., V. Chandrasekar, N. Balakrishnan and D.S. Zrnic, 1990: An Examination of Propagation Effects in Rainfall on Radar Measurements at Microwave Frequencies. *J Atmos Oceanic Tech.* Vol. 7, pp. 829–840.

Bringi, V.N., K. Knupp, A. Detwiler, L. Liu, I.J. Caylor and R.A. Black, 1997: Evolution of a Florida Thunderstorm during the Convection and Precipitation/Electrification Experiment: The Case of 9 August 1991. *Mon. Wea. Rev.* Vol. 125, pp 2131–2160

Bringi, V.N. and M. Thurai, 2008: Preliminary assessment and analysis of the CP2 S&X band data, Internal report for the Centre for Australian and Climate research, Melbourne, AU.

Eccles, P.J. and E.A Mueller, 1972: X-Band Attenuation and Liquid Water Content Estimation by a Dual-Wavelength Radar. *J Appl. Meteor.* Vol. 10, pp 1252–1259.

Hitschfeld, W., and J. Bordan, 1954: Errors inherent in the radar measurement of rainfall at attenuating wavelengths., *J. Meteor.,* Vol. 11, 58-67.

Hubbert, J., and V.N. Bringi, 1995: An iterative filtering technique for the analysis of copolar differential phase and dual-frequency radar measurements., *J. Atmos. Oceanic Technol.,* Vol. 12, 643-648

Knight, C.A. and L. Jay Miller, 1998: Early Radar Echoes from Small, Warm Cumulus: Bragg and Hydrometeor Scattering. *J Atmos Sci.,* Vol. 55, pp 2974–2992.

Leon, L., G.J. Huang, Y. Liu, V.N. Bringi and A.M. loftus, 2007: Rain and wet hail specific attenuation estimation for a 3D supercell case using RAMS model to simulate CASA X-band and WSR-88D S-band radar signals. *Proc. 33rd Conf. Radar Meteor.,* P11B.10, AMS, Cairns, 5-10 August.

Tuttle, J.D., and R.E. Rinehart, 1983: Attenuation correction in dual-wavelength analyses., *J. Climate Appl. Meteor.,* Vol. **22**, 1914-1921.